Biotechnol Lett (2024) 46:213–221
https://doi.org/10.1007/s10529-023-03450-3

ORIGINAL RESEARCH PAPER

Performance of a combined electrotrophic and electrogenic biofilm operated under long-term, continuous cycling

Matthew D. Yates · Rebecca L. Mickol · Amelia Vignola · Jeffrey W. Baldwin · Sarah M. Glaven · Leonard M. Tender

Received: 21 July 2023 / Revised: 14 October 2023 / Accepted: 4 November 2023 / Published online: 1 February 2024

Abstract
Objectives Evaluate electrochemically active biofilms as high energy density rechargeable microbial batteries toward providing persistent power in applications where traditional battery technology is limiting (, remote monitoring applications).
Results Here we demonstrated that an electrochemically active biofilm was able to store and release electrical charge for alternating charge/discharge cycles of up to 24 h periodicity (50% duty cycle) with no significant decrease in average current density (0.16 ± 0.04 A/m^2) for over 600 days. However, operation at 24 h periodicity for > 50 days resulted in a sharp decrease in the current to nearly zero. This current crash was recoverable by decreasing the periodicity. Overall, the coulombic efficiency remained near unity within experimental error ($102 \pm 3\%$) for all of the tested cycling periods. Electrochemical characterization here suggests that electron transfer occurs through multiple routes, likely a mixture of direct and mediated mechanisms.
Conclusions These results indicate that bidirectional electrogenic/electrotrophic biofilms are capable of efficient charge storage/release over a wide range of cycling frequency and may eventually enable development of sustainable, high energy density rechargeable batteries.

Keywords Bioelectrochemistry · Biofilm · Energy storage · Extracellular electron transfer

Introduction

Bacterial biofilms are functional materials with the potential to enable technologies that significantly reduce anthropogenic impact on the environment. Certain bacterial biofilms, for example, can perform the charge storage and release functions of batteries, utilizing electrodes as electron sources or sinks for electron-consuming (electrotrophic (Summers et al. 2013)) or electron-generating (electrogenic (Logan et al. 2019)) metabolic processes. Moreover, these processes involve reduction of carbon dioxide (CO_2) to form organic compounds that store electrons (Eddie et al. 2017; Jourdin et al. 2015) and oxidation of organic compounds that release electrons (Logan 2009). This ability to store and release electrons and

Supplementary Information The online version contains supplementary material available at https://doi.org/10.1007/s10529-023-03450-3.

M. D. Yates (✉) · R. L. Mickol · S. M. Glaven · L. M. Tender
Center for Bio/Molecular Science and Engineering, Naval Research Laboratory, Washington, DC 20375, USA
e-mail: matthew.yates@nrl.navy.mil

L. M. Tender
e-mail: leonard.tender@nrl.navy.mil

A. Vignola · J. W. Baldwin
Acoustics Division, Naval Research Laboratory, Washington, DC 20375, USA

CO_2 could be used as the basis for microbial-based batteries that may potentially have advantages over conventional batteries, such as increased operational lifetime, especially in situations where system maintenance is logistically challenging, as in the case of remote monitoring applications that require constant low power.

As a proof of concept, we previously demonstrated enrichment of a microbial mixed community electrode-grown biofilm originating from river sediment that is uniquely adept at both storing and subsequently releasing electrons with the electrode acting as the electron source or sink depending upon the applied potential. The biofilm, called the CANode (Cathode–ANode), is electrotrophic (charge storage) at −0.4 V vs. standard hydrogen electrode (V_{SHE}) and electrogenic (charge release) at 0 V_{SHE} (Yates et al. 2017). The cathodic and anodic currents associated with the alternating charging and discharging cycles of 0.33 h with a 50% duty cycle (i.e., 0.17 h storage and 0.17 h release) increased in lock step over time following inoculation, consistent with a living biofilm underlying the charge storage and release, i.e., cellular metabolic processes are catalyzing electron exchange with the electrode. Moreover, the amount of charge released during a given discharge cycle equaled the amount stored during the previous charge cycle within experimental error even after continuous cycling for over a year. This suggests that the microbial mechanisms underlying charging and discharging are somehow coupled and robust. Recent metagenomic and metatranscriptomic analyses of a similar CANode biofilm indicated that the metabolic processes occurring are likely a complex combination of electron transfer processes, such as hydrogen via hydrogenases, sulfur via sulfate reduction, ethanol via CO_2 reduction, and direct contact via *c*-type cytochromes expressed by multiple organisms (Mickol et al. 2021). Further, the differential gene expression analysis suggested that CO_2/ethanol and sulfate/sulfide were major species being oxidized and reduced within the biofilm (Mickol et al. 2021; Thorup et al. 2017). Additionally, recent electrochemical characterizations of the bidirectional electron transfer capabilities of closely-related members of the CANode community in pure culture (*Desulfarculus baarsii*, the closest relative to the most abundant organism in the CANode biofilm) and *Desulfurivibrio alkaliphilus* (the closest relative to the most active organism in the CANode biofilm (Mickol et al. 2021)) indicated that sulfur cycling may play a role in biofilms capable of bidirectional electron transfer (Izadi and Schröder 2022).

Here, we characterized the electron transfer and storage characteristics of the CANode biofilm for over 600 days with periodicity up to 24 h with a 50% duty cycle to determine the capabilities of the biofilm when operated under longer cycling periods that are more likely to be encountered in an operational setting (i.e., remote power for sensing and monitoring devices). In prior work, the CANode biofilm had only been operated for ca. 100 days with a periodicity of 0.33 h. Here we show that this biofilm is able to operate with significantly longer periodicities for extended periods of time. These fundamental insights into the electron transfer processes occurring in the CANode biofilm will help enable the development of sustainable energy storage and conversion technologies based on self-sustaining microbial biofilms.

Materials and methods

Reactor construction

Dual-chambered reactors (n = 6) were set up as previously described, with minor differences in the reactor architecture (Yates et al. 2017). The volume of each chamber was 260 mL (60 mL headspace). The working electrode consisted of HCl-treated carbon cloth (5 cm × 5 cm) attached to a titanium wire with a titanium nut and bolt. The counter electrode was platinum mesh attached to a titanium wire. The reference electrode was Ag/AgCl [3 M NaCl; + 0.21 V_{SHE}]. The two chambers were separated by a cation exchange membrane (CMI-7000, Membranes International). The reactors were stirred at 200 rpm, not temperature-controlled (ambient temperature ranged from 23 to 25 °C), and covered with cloth to reduce light exposure. Reactors were filled with 200 mL sterile, anaerobic, CO_2-buffered artificial seawater medium (ASW) (Schübbe et al. 2009) per chamber (400 mL per reactor). The artificial seawater medium contained (per liter): 27.5 g NaCl, 3.8 g $MgCl_2 \cdot 6H_2O$, 6.78 g $MgSO_4 \cdot 7H_2O$, 0.72 g KCl, 0.62 g $NaHCO_3$, 2.79 g $CaCl_2 \cdot 2H_2O$, 1 g NH_4Cl, 0.05 g K_2HPO_4, and 1 mL Wolfe's Trace Mineral Solution ([per liter]: 1.5 g nitrilotriacetic acid, 3 g $MgSO_4 \cdot 7H_2O$, 0.5 g

$MnSO_4 \cdot H_2O$, 1 g NaCl, 0.1 g $FeSO_4 \cdot 7H_2O$, 0.1 g $CoCl_2 \cdot 6H_2O$, 0.1 g $CaCl_2$, 0.1 g $ZnSO_4 \cdot 7H_2O$, 0.01 g $CuSO_4 \cdot 5H_2O$, 0.01 g $AlK(SO_4)_2 \cdot 12H_2O$, 0.01 g H_3BO_3, 0.01 g $Na_2MoO_4 \cdot 2H_2O$). No organic carbon was added to the reactor as an energy or carbon source for growth. The oxygen was removed from the medium and the pH was adjusted to 6.4 after autoclaving by sparging with a stream of sterile 80%/20% N_2/CO_2 gas mix. Reactors were filled with sterile, anaerobic ASW in an anaerobic glove box (Coy Laboratories), then flushed with 0.22 µm-filtered 80%/20% N_2/CO_2 gas for ten minutes upon returning to the stir plate. The initial medium pH was 6.4.

Reactor inoculation and operation

The CANode biofilms investigated here are 3rd generation enrichments inoculated from biofilm scrapings from the working electrodes of the previous generation of enrichments (Yates et al. 2017). The inoculum for these reactors was obtained by removing a 3 cm^2 piece of the carbon cloth working electrode from two 2nd generation reactors (Yates et al. 2017) with a sterile razor blade in a sterile petri dish inside of an anaerobic chamber. The cloth was cut into small pieces and added to two 50-mL centrifuge tubes containing 30 mL spent reactor medium each. The tubes were shaken by hand and the liquid was transferred back and forth between the two tubes to homogenize the inoculum. The six reactors were each inoculated with 10 mL of this suspension using a sterile syringe and needle. After inoculation, both chambers were flushed with 0.22 µm-filtered 80%/20% N_2/CO_2 gas for 10 min to remove residual oxygen. The working electrode potential was then alternated between 0.0 V_{SHE} and −0.4 V_{SHE} every ten minutes (0.33 h cycling period) using a multichannel potentiostat (VMP3, BioLogic) based on the potentials used for the original enrichment (Yates et al. 2017). After the current stabilized (< 30 days compared to 156 days for 1st generation CANode biofilms (Yates et al. 2017)), the cycling period was successively changed between 0.33, 1, 2, 6, 24, then 4 h, each with a 50% duty cycle. A 0.33 h cycling period is defined as the baseline (Mickol et al. 2021; Yates et al. 2017). The average stable current density (0.16 ± 0.02 A/m^2) produced during the baseline 0.33 h cycling period was approximately three times less than that produced by the 2nd generation CANode biofilms with the same cycling period (Yates et al. 2017). Reasons for this are unclear as all operational parameters and procedures were the same as for previous reactors and may reflect slight differences in the reactors used here.

Insights into biofilm processes were obtained by performing chronoamperometry (CA), cyclic voltammetry (CV), and square wave voltammetry (SWV) for the various cycle lengths. For CV, potentials were scanned between 0.6 and −0.45 V_{SHE} at 1 mV/s. SWV was performed over the same potential range with a 25 mV pulse height, a 250 ms pulse width, and a 0.5 mV step size. Voltammetry was not performed for the 24 or 4 h cycling periods due to a sudden decrease in the current to near zero during the 24 h periodicity, which preceded the 4 h periodicity.

Data processing and calculations

A custom Matlab (Mathworks, USA) script was written to sort all data from different files by time then remove the large transient spike in current, which is attributed to capacitance charging (Yates et al. 2017), following each potential change to more easily visualize the remaining steady-state current data. The data were not processed further after removal of the large transient (i.e., data points in Fig. 1a or Fig. S1 are not averages of multiple points). The script also calculated the coulombic efficiency for the total operation of each reactor and for each individual cycling period, and calculated the average current density for each charge/discharge cycle for comparisons across periodicities. The data were plotted using OriginPro (Origin Labs, USA). The accumulated charge was determined by the following equation:

$$Total\,Accumulated\,Charge = 1 - \frac{\sum_0^t Q}{\sum_0^t |Q|}$$

where Q is the charge and |Q| is the magnitude (absolute value) of the charge at a given point in time. Imbalances in the cathodic and anodic charge will cause the total accumulated charge to deviate from unity.

Headspace gas composition and pH analyses

Headspace gas samples were taken periodically both prior to and following inoculation using sterile needles and gas-tight syringes and analyzed via gas

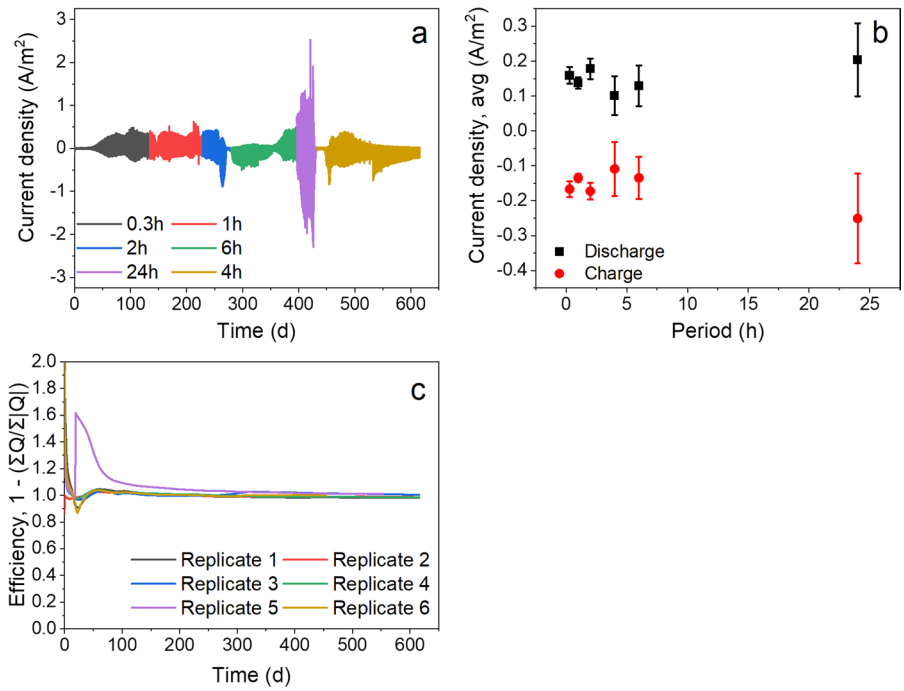

Fig. 1 Electrochemical characterization of the CANode biofilms. **a** Raw chronoamperometry data from one CANode biofilm with the large current transients removed. **b** Average anodic and cathodic currents within each cycling periodicity. Representative magnified raw current data can be found in Fig. S2. Data from replicates can be found in Fig. S1–S4. The color scheme used here corresponds to the different cycling periodicities tested and is consistent throughout the figures. **c** Cumulative reactor efficiency over time. Each point represents the ratio of the cumulative charge to the absolute value of the cumulative charge, indicating how much of the charge is conserved between anodic and cathodic operation over time

chromatography (Peak Laboratories) for hydrogen, carbon monoxide, methane, and oxygen (carrier gas: ultra-high purity N_2). Methane and oxygen were not detected in reactors throughout the experiment. Five-milliliter aliquots of medium from the working electrode chamber were removed periodically in order to measure pH. Sterile, anaerobic ASW medium was added back to each reactor to replace the medium removed.

Results and discussion

Effects of increasing the cycling periodicity up to 24 h

As observed for previous generation CANode biofilms, cathodic and anodic current produced by these 3rd generation CANode biofilms (Fig. 1a, Fig. S1, n = 6) increased in lock step following reactor inoculation in response to stepping the applied potential repeatedly between −0.4 and 0 V_{SHE} to alternatively favor electrotrophy (charge storage) and electrogenesis (charge release) at 0.33 h periodicity and 50% duty cycle. At up to 1 h periodicity (50% duty cycle) CANode biofilms can be charged and discharged for at least 250 days with 102 ± 4% coulombic efficiency (Fig. 1a). Further increasing the cycling periodicity to 2, 6, 24, and then a decrease to 4 h did not statistically (t-test, $p > 0.05$) change the average cathodic or anodic current density of charging and discharging cycles (Fig. 1b) compared to the baseline (defined as 0.33 h periodicity). Previous CANode biofilms were operated for a maximum of 100 days at 0.33 h periodicity. Our results here indicate a reversible biofilm is capable of operating over six times longer with a ten times increase in periodicity than previously demonstrated. However, we also noted that occasional imbalances in anodic and cathodic currents appeared more frequently with increasing periodicity (Fig. 1a). At periodicities less than 24 h, these imbalances were temporary and recoverable and

the coulombic efficiency (Fig. 1C) was unaffected. Charging and discharging currents of five replicates rapidly decreased below 0.01 A/m^2 when a 24 h periodicity was applied (Fig. S1), with a similar decrease in current for one replicate during the 6 h periodicity. However, all eventually recovered back to previous levels (0.1 ± 0.05 A/m^2) after the cycling period was decreased back to 4 h (Fig. 1a, S1). Prior to the rapid decrease in current, there was a large increase in the maximum current density (to ~ 0.4 A/m^2) at the start of each cycle in three of the five reactors when the periodicity was first switched to 24 h. However, that increase was temporary as the overall average current density at 24 h periodicity was not statistically larger than other periodicities (Fig. 1b). Further inspection of the individual charge/discharge cycles (Fig. S2) shows the transient nature of these increases in maximum current density. The temporary increase in current may reflect more available reduced carbon during anodic operation due to a longer accumulation time during cathodic operation. The cause of the rapid decrease to near-zero current density is currently unknown, but the initial increase in current (although temporary) indicates that the output of the biofilm can be significantly enhanced by further optimization of the reactor conditions. Interestingly, the chronoamperometry data indicate a sharp decrease in the cathodic current in each of the reactors followed by a subsequent sharp decrease of the anodic current. This rapid decline in cathodic current may be a result of an accumulation of compounds to inhibitory levels, such as ethanol and/or sulfide produced from the oxidation of ethanol coupled to the reduction of sulfate (Mickol et al. 2021), produced during cathodic operation at extended periodicities. Nonetheless, the coulombic efficiency was unity within experimental error ($102 \pm 3\%$, $n = 6$) over the nearly 600 days of continuous operation (Fig. 1c), as can be seen from the accumulation of charge over time. The step deviation observed in Replicate 5 was due to a loose electrode connection. As more data were collected, this deviation was averaged out over time. Interestingly, a distinct current profile was observed during operation at different periodicities (Fig. S2), especially during the cathodic portion of the cycle. While it is difficult to ascribe an exact mechanism from the CA data, it does indicate that there is a complex dynamic occurring in the system. Taken together, these data highlight the efficiency of the processes occurring in this microbial community over extended periods of operation, which is critical for implementation of this technology outside of the laboratory. Future experimentation with this system should consider utilizing different duty cycles to attempt to maximize the charge storage and release without the observed rapid decrease in current and to understand more precisely the processes occurring in the biofilm.

Voltammetry indicates reversible redox activity

Square wave voltammograms (SWV; Fig. 2a, Fig. S3) taken throughout the experiment exhibit peak(s) that mirror during oxidative and reductive scans, indicating a reversible electron transfer process is taking place in the biofilm at each periodicity. SWVs taken during 0.33 and 1 h cycling periodicity revealed

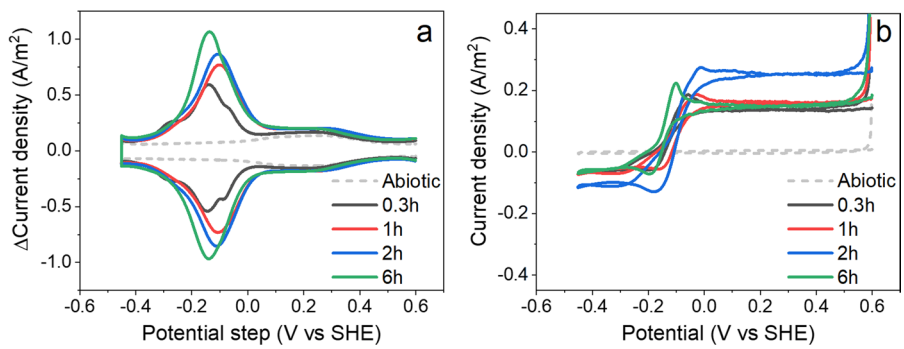

Fig. 2 Voltammetry data from CANode biofilms, including **a** Square wave voltammograms of the CANode biofilm taken at different periodicities. **b** Cyclic voltammograms taken for different periodicities. Voltammograms shown are from the reactor depicted in Fig. 1a. Data from replicates can be found in Fig. S1–S4. The color scheme used here corresponds to the different cycling periodicities tested and is consistent throughout the figures

multiple overlapping peaks centered at −0.13 V_{SHE}, similar in curve shape and potential to what has been attributed to *c*-type cytochromes in *Geobacter* electroactive biofilms (Liu et al. 2011) and in curve shape to what has been observed for a microbial biocathode (Yates et al. 2016). Such overlapping peaks may reflect a single redox cofactor in different microenvironments or multiple different cofactors, each resulting in distinct formal potentials, able to directly engage in bidirectional electron transfer across the biofilm/electrode interface that mediates the charging and discharging processes (Gulaboski et al. 2019). Further evidence for *c*-type cytochromes acting as EET conduits comes from the high abundance of these proteins identified as being expressed by multiple members of the CANode biofilm community in a previous metatranscriptomic characterization (Mickol et al. 2021). In particular, the *Desulfobulbaceae* deemed to be responsible for a majority of the current production contained 185 predicted hypothetical or cytochrome *c* family proteins with at least one covalently bound heme (Mickol et al. 2021). Alternatively, the SWV may reflect an extracellular enzyme(s) (i.e., enzyme(s) not associated with a cell), such as a hydrogenase, that can engage in bidirectional electron transfer directly with the electrode (Smith et al. 2001) and mediates electron flow to (Deutzmann et al. 2015; Yates et al. 2014) and from (Joshi et al. 2019) cells in the CANode biofilm during charging and discharging. Further, the presence of reversible redox mediators could enable capacitive charge storage (Heijne et al. 2018) and release mechanism in the biofilms under study here. For longer cycling periodicities, SWVs exhibit an increase in the peak anodic and cathodic current, suggesting that either the abundance of redox cofactors (or extracellular enzymes) that mediate the heterogeneous electron transfer reaction or the diffusion coefficient for charge transfer in the biofilm, or both, increases over time (Otero et al. 2021). In addition, SWVs converge to a single peak for longer cycling periodicity, suggesting that the nature of the heterogeneous electron transfer reaction itself changes, likely reflecting a more uniform pool of mediators and/or an increase in the concentration of the redox mediator.

Cyclic voltammetry (CV, Fig. 2b, Fig. S4) reveals a single bidirectional catalytic wave, similar to those observed for reversible enzyme electrocatalysts (Armstrong and Hirst 2011) with a midpoint potential that aligns with the SWV peaks, consistent with the charging and discharging abilities of the CANode biofilm for either redox cofactor-mediator scenario described above. Despite the apparent increase in abundance of redox cofactor involved in heterogeneous electron transfer over time or with increasing periodicity, CV indicates that the CANode biofilm sustains the highest limiting catalytic current for a 2 h cycling period. However, there did not seem to be a significant trend in the limiting current of the CV over different applied periodicities, further highlighting the stability of the system performance with regards to electrochemical characteristics over the course of the experiment. The limiting cathodic current during CV was only 50% of the limiting anodic current during CV, different from the previously observed 1:1 anodic:cathodic limiting current (Yates et al. 2017). This also contrasts with the 1:1 anodic:cathodic current observed during the course of the chronoamperometry. We currently ascribe this to oxidation of molecules generated during cathodic operation at potentials that are only applied during voltammetry. Lower cathodic current indicates that these compounds that are oxidized cannot be regenerated at the same rate during cathodic portions of the scan, however more tests are needed to confirm this hypothesis. This imbalance may also suggest a buildup of reduced carbon in the reactor due to longer operational time as a cathode resulting in increased anodic current. Previous work investigating bidirectional electron transfer in bacterial biofilms, both mixed (Izadi et al. 2021) and pure culture (Izadi and Schröder 2022), observed a strong signal during voltammetry due to electrochemical cycling of biogenic sulfur compounds. However, the voltammetry here indicated that sulfur cycling was unlikely a dominant heterogeneous electron transfer process in the system (i.e., the process that mediates transfer of electrons at the interface of the electrode and the biofilm (Yates et al. 2018)). However, a previous analysis of the CANode community (Mickol et al. 2021) suggests sulfur cycling may play a role in homogeneous electron transfer (i.e., electron transfer within the biofilm (Yates et al. 2015)) here.

pH and headspace gas composition analysis

Gaseous electron donors, specifically H_2 and CO, are well-known substrates in anaerobic systems (Jourdin et al. 2016; Oelgeschläger and Rother 2008) and

were monitored periodically here to determine their potential role in these reactors. The concentration of H_2 and CO in the headspace of the working electrode half-cell generally remained at concentrations below the detection limit of our gas chromatograph throughout the experiment (~0.1 ppm). Carbon monoxide was detected in small amounts (<4 ppm, Fig. 3a) on three occasions in one of the six replicates. Hydrogen, on the other hand, was detected in variable amounts between 0.1 and 495 ppm at irregular intervals throughout the experiment (Fig. 3a). We cannot exclude the potential for CO production due to degradation of the carbon electrode itself, as previously shown in a similar system (Siegert et al. 2014). When the working electrode was operated as an anode during charging, the abiotic Pt counter electrode may reduce protons to H_2. We cannot rule out that counter electrode-generated H_2 could be utilized by the CANode biofilm as an electron donor (or oxidized by a hydrogenase residing at the electrode surface—bypassing the biofilm entirely), resulting in an increase in discharging current in a generator-collector configuration driven by the applied potential to the working electrode (Joshi et al. 2019). This would require H_2 to diffuse ca. 11 cm from the counter electrode half-cell through the membrane to the working electrode—a scenario we deem unlikely to make significant contributions to charge transfer in the reactors.

The presence of H_2, albeit at low concentrations, could result from its generation at the working electrode during charging, mediated either by a hydrogenase (or similar electrode-associated enzyme), non-viable cell material (Yates et al. 2014), or directly by the electrode, which occurs near −0.4 V_{SHE} (Siegert et al. 2014). However, we note that the specific reactor conditions and the specific mechanism used will dictate the potential at which H_2 is generated. Given the uniform nature of the SWV, which most likely reflects only one mechanism of heterogeneous electron transfer, especially at longer periodicity, we contend that the heterogeneous electron transfer reaction is predominately mediated by a redox cofactor and not H_2. In this scenario, H_2 would be generated as secondary product directly by the electrode during charging at a low enough rate (consuming a small enough fraction of electrons passed during charging) as to not obscure the SWV, which would otherwise reflect the irreversibility of H_2 generated directly by the electrode. Moreover, a fraction of electrode-generated H_2 could be consumed during charging, however that electrochemically-derived H_2 fraction is not sufficient enough to affect the overall charging/discharging coulombic efficiency. At longer cycling periodicities (i.e., 24 h), H_2 would have a longer time to accumulate and could contribute to the increase in current density by providing additional substrate for conversion to other metabolites (Mickol et al. 2021). However, CO_2 is not being added into the reactors continuously during these experiments, which could limit the conversion of H_2 into organic compounds, such as ethanol (Mickol et al. 2021), and ultimately prevent detection of these metabolites via standard analytical methods. The stability of the medium pH was monitored throughout the experiment and was

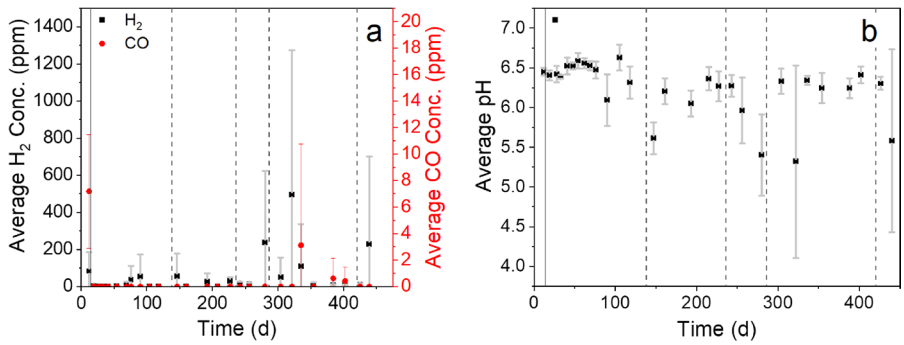

Fig. 3 **a** Gas chromatograph data showing the average (n = 6) amount of hydrogen (H_2, black squares) and carbon monoxide (CO, red circles) detected in the headspace of the working electrode half-cell over time. **b** Average (n = 6) reactor pH throughout the duration of the experiment. The solid line on day 13 indicates when the reactors were inoculated. Dashed lines indicate changes in cycling period. Medium exchanges were performed on days 133, 202, 228, 286, 344, and 420 (not shown)

found to remain primarily near the starting pH of the medium (around 6.4) with a few excursions to close to 5.5 (Fig. 3b), suggesting overall reactions that were pH-neutral (i.e., protons were balanced overall in reactions occurring within the CANode biofilm). This indicates that protons consumed while charging during cathodic operation were liberated while discharging during anodic operation, which kept an overall stable pH in the system. We note that the variability in the pH for two time points indicated a significant drop in the pH of one reactor. We did not notice a concomitant decrease in the current and the pH returned to typical values without intervention.

Conclusions

Here we show that a bidirectional electroactive biofilm can be operated as an alternating anode and cathode for extended periods of time (> 600 days) under different cycling periods of up to 24 h (50% duty cycle). The biofilm was able to maintain a characteristic sigmoidal curve that spanned positive and negative currents despite being operated under cycling periods ca. 20× longer than the baseline conditions used to enrich the biofilm. Remarkably, the total coulombic efficiency remained at unity, within experimental error, over the entirety of the experimental period. Further, the electrochemical data obtained under these conditions indicate that a single redox mediator (or multiple redox mediators with similar formal potentials) is responsible for the majority of the observed current from the biofilm. Interestingly, we did not detect electrochemical signatures from cycling of sulfur compounds despite previous metagenomic and metatranscriptomic evidence that sulfur species likely play an important role in the metabolic processes occurring among the biofilm constituents. The seemingly complicated electron transfer processes occurring in the biofilm, especially regarding the metabolites generated and utilized during operation of the CANode, remain open questions about our fundamental understanding of bidirectional electroactive biofilms. Despite these outstanding knowledge gaps, the results presented here lay the groundwork for development of sustainable energy storage and conversion technologies, such as batteries that can be utilized for monitoring remote locations.

Acknowledgements This work was supported by NRL internal base program funding.

Author contributions Sample collection and data analysis was performed by MY, RM, and AV. JB, SG, and LT were responsible for funding acquisition and supervision. LT and MY were responsible for conceptualization of the experiments. All authors were involved with writing and editing the final approved manuscript.

Funding This study was supported by US Naval Research Laboratory, Internal Base Funding.

Declarations

Competing interests The Authors declare no competing interests.

References

Armstrong FA, Hirst J (2011) Reversibility and efficiency in electrocatalytic energy conversion and lessons from enzymes. Proc Natl Acad Sci USA 108:14049–14054

Deutzmann JS, Sahin M, Spormann AM (2015) Extracellular enzymes facilitate electron uptake in biocorrosion and bioelectrosynthesis. Mbio 6:e00496-e515

Eddie BJ, Wang Z, Hervey WJT, Leary DH, Malanoski AP, Tender LM, Lin B, Strycharz-Glaven SM (2017) Metatranscriptomics supports the mechanism for biocathode electroautotrophy by "*Candidatus* Tenderia electrophaga." mSystems 2:e00002-17

Gulaboski R, Mirceski V, Lovric M (2019) Square-wave protein-film voltammetry: new insights in the enzymatic electrode processes coupled with chemical reactions. J Solid State Electr 23:2493–2506

Izadi P, Schröder U (2022) What is the role of individual species within bidirectional electroactive microbial biofilms: a case study on *Desulfarculus baarsii* and *Desulfurivibrio alkaliphilus*. ChemElectroChem 9:e202101116

Izadi P, Gey MN, Schlüter N, Schröder U (2021) Bidirectional electroactive microbial biofilms and the role of biogenic sulfur in charge storage and release. iScience 24:102822

Joshi K, Kane AL, Kotloski NJ, Gralnick JA, Bond DR (2019) Preventing hydrogen disposal increases electrode utilization efficiency by *Shewanella oneidensis*. Front Energ Res. https://doi.org/10.3389/fenrg.2019.00095

Jourdin L, Grieger T, Monetti J, Flexer V, Freguia S, Lu Y, Chen J, Romano M, Wallace GG, Keller J (2015) High Acetic Acid Production Rate Obtained by Microbial Electrosynthesis from Carbon Dioxide. Environ Sci Technol 49:13566–13574

Jourdin L, Lu Y, Flexer V, Keller J, Freguia S (2016) Biologically induced hydrogen production drives high rate/high efficiency microbial electrosynthesis of acetate from carbon dioxide. ChemElectroChem 3:581–591

Liu Y, Kim H, Franklin RR, Bond DR (2011) Linking spectral and electrochemical analysis to monitor *c*-type cytochrome redox status in living *Geobacter sulfurreducens* biofilms. ChemPhysChem 12:2235–2241

Logan BE (2009) Exoelectrogenic bacteria that power microbial fuel cells. Nat Rev Microbiol 7:375–381

Logan BE, Rossi R, Aa R, Saikaly PE (2019) Electroactive microorganisms in bioelectrochemical systems. Nat Rev Microbiol 17:307–319

Mickol RL, Eddie BJ, Malanoski AP, Yates MD, Tender LM, Glaven SM (2021) Metagenomic and metatranscriptomic characterization of a microbial community that catalyzes both energy-generating and energy-storing electrode reactions. Appl Environ Microbiol 87:e0167621

Oelgeschläger E, Rother M (2008) Carbon monoxide-dependent energy metabolism in anaerobic bacteria and archaea. Arch Microbiol 190:257–269

Otero FJ, Chadwick GL, Yates MD, Mickol RL, Saunders SH, Glaven SM, Gralnick JA, Newman DK, Tender LM, Orphan VJ, Bond DR (2021) Evidence of a streamlined extracellular electron transfer pathway from biofilm structure, metabolic stratification, and long-range electron transfer parameters. Appl Environ Microbiol 87:e00706-e721

Schübbe S, Williams TJ, Xie G, Kiss HE, Brettin TS, Martinez D, Ross CA, Schüler D, Cox BL, Nealson KH, Bazylinski DA (2009) Complete genome sequence of the chemolithoautotrophic marine magnetotactic coccus strain MC-1. Appl Environ Microbiol 75:4835–4852

Siegert M, Yates MD, Call DF, Zhu X, Spormann AM, Logan BE (2014) Comparison of non-precious metal cathode materials for methane production by electromethanogenesis. ACS Sus Chem Eng 2:910–917

Smith ET, Odom LD, Awramko JA, Chiong M, Blamey J (2001) Direct electrochemical characterization of hyperthermophilic *Thermococcus celer* metalloenzymes involved in hydrogen production from pyruvate. J Biol Inorg Chem 6:227–231

Summers ZM, Gralnick JA, Bond DR (2013) Cultivation of an obligate Fe(II)-oxidizing lithoautotrophic bacterium using electrodes. Mbio 4:e00420-e512

Ter Heijne A, Liu D, Sulonen M, Sleutels T, Fabregat-Santiago F (2018) Quantification of bio-anode capacitance in bioelectrochemical systems using electrochemical impedance spectroscopy. J Power Sour 400:533–538

Thorup C, Schramm A, Findlay AJ, Finster KW, Schreiber L, Newman DK (2017) Disguised as a sulfate reducer: growth of the deltaproteobacterium *Desulfurivibrio alkaliphilus* by sulfide oxidation with nitrate. Mbio 8:e00671-e717

Yates MD, Siegert M, Logan BE (2014) Hydrogen evolution catalyzed by viable and non-viable cells on biocathodes. Int J Hydrogen Energ 39:16841–16851

Yates MD, Golden JP, Roy J, Strycharz-Glaven SM, Tsoi S, Erickson JS, El-Naggar MY, Calabrese Barton S, Tender LM (2015) Thermally activated long range electron transport in living biofilms. Phys Chem Chem Phys 17:32564–32570

Yates MD, Eddie BJ, Kotloski NJ, Lebedev N, Malanoski AP, Lin BC, Strycharz-Glaven SM, Tender LM (2016) Toward understanding long-distance extracellular electron transport in an electroautotrophic microbial community. Energ Environ Sci 9:3544–3558

Yates MD, Ma L, Sack J, Golden JP, Strycharz-Glaven SM, Yates SR, Tender LM (2017) Microbial electrochemical energy storage and recovery in a combined electrotrophic and electrogenic biofilm. Environ Sci Technol Lett 4:374–379

Yates MD, Eddie BJ, Lebedev N, Kotloski NJ, Strycharz-Glaven SM, Tender LM (2018) On the relationship between long-distance and heterogeneous electron transfer in electrode-grown *Geobacter sulfurreducens* biofilms. Bioelectrochemistry 119:111–118